PNAS RESEARCH ARTICLE | EVOLUTION

When islands collide: Divergence predicts outcomes of secondary contact during the fusion of Sulawesi's paleo-archipelago

Benjamin R. Karin[a,b,1,2], Jeffrey H. Frederick[a,3], Amir Hamidy[c], Awal Riyanto[c], Evy Arida[d], Djoko T. Iskandar[e,f], Indraneil Das[g], Adi Shabrani[g,h,i], Evan S. H. Quah[j,k], Todd R. Jackman[b], Aaron M. Bauer[b], and Jimmy A. McGuire[a]

Affiliations are included on p. 11.

Edited by David Hillis, The University of Texas at Austin, Austin, TX; received June 11, 2025; accepted September 15, 2025

Speciation often results from the accumulation of reproductive isolation associated with lineage divergence, but secondary contact between diverged lineages can reshape the trajectory of speciation and reveal its underlying processes. The Indonesian island of Sulawesi is a tectonically complex island formed by the fusion of many paleo-islands, resulting in replicated cases of secondary contact among once-isolated lineages. Unlike secondary contact on continents where hybridization often results from unpredictable range shifts, Sulawesi's fauna presents a replicated set of geologically constrained natural experiments to test how the magnitude of evolutionary divergence predicts outcomes of secondary contact and hybridization. Using thousands of genome-wide loci from *Eutropis* sun skinks spanning Wallace's Line on Sulawesi and Borneo, we reconstructed a reticulate evolutionary history shaped by overwater dispersal, isolation, island fusion, hybridization, and character displacement. We delimited five distinct species (three undescribed) and uncovered multiple ancient hybridization events following island fusion leading to distinct outcomes. These outcomes—speciation reversal, parapatry, and sympatry putatively through reproductive character displacement—were associated with increasing levels of prior divergence consistent with evolutionary theory. Sympatry, specifically, was preceded by substantial introgressive hybridization and body size divergence that likely confers reproductive incompatibility. Together, these results provide empirical support for divergence-dependent tipping points along the speciation continuum. The sun skink radiation also includes a rare instance of reverse colonization of Borneo across Wallace's Line that established a narrowly divergent species with a uniquely intermediate body size absent from Sulawesi.

speciation | lizard | character displacement | phylogenomics | Wallace's Line

Significance

Natural experiments that test species boundaries can reveal key insights into how biodiversity is generated and maintained. Sulawesi, formed by the fusion of formerly isolated paleo-islands that brought populations into secondary contact, provides a rare opportunity to test whether the outcomes are predictable. When Sulawesi fused, previously isolated sun skink populations displayed distinct outcomes—from merger, to contact zones, to full sympatry—contingent on the time of isolation. Other fauna on Sulawesi share a subset of these outcomes, but apparently only sun skinks achieved sympatry by diverging in body size, highlighting how physical traits maintain species boundaries. These results provide real-world support for core predictions of evolutionary theory and show how Earth's geological history continues to shape biodiversity.

Elucidating and characterizing the processes underpinning speciation is a fundamental goal of biodiversity science. Many species are completely reproductively isolated from close relatives, either by intrinsic reproductive isolating mechanisms or geographic separation (1). However, there are also species with incomplete reproductive isolation, and investigating these lineages can shed important light on fundamental aspects of the speciation process (2). The early stages of lineage divergence often occur in geographic isolation due to drift where genetic differences and reproductive incompatibilities accumulate (3). A critical junction in this process occurs if these diverging lineages meet in secondary contact following isolation. This secondary contact may lead to genetic exchange that can cause the process to either reverse, proceed, or even accelerate (4). Secondary contact provides a natural test of the degree of established reproductive isolation and can produce an array of outcomes that offer insights into the origins and maintenance of biodiversity (5).

Evolutionary theory and empirical studies suggest that the consequences of secondary contact are contingent on the extent of genetic divergence between the interacting lineages (6–10). If divergence is limited and reproductive barriers are weak, extensive hybridization and gene flow can lead to the collapse of incipient species boundaries—reversed (11) or arrested speciation (12) (Fig. 1*A*). Conversely, at moderate levels of genetic divergence, lineages may maintain their distinctiveness despite significant gene flow (2). This can result in stable hybrid zones where lineages meet but interbreed sparingly (parapatry), or even progress toward coexistence in the same geographic area (sympatry) (2) (Fig. 1*A*). Sympatry between closely related species is assumed to require strong pre- or postzygotic isolation mechanisms, as otherwise their species boundaries would collapse (1). Secondary contact can also accelerate speciation either by directly generating reproductively isolated hybrid

This article is a PNAS Direct Submission.

PNAS policy is to publish maps as provided by the authors.

[1]To whom correspondence may be addressed. Email: benkarin@berkeley.edu.

[2]Present address: Department of Environmental Science, Policy, and Management, University of California, Berkeley, CA 94720.

[3]Present address: Department of Biology, University of Kentucky, Lexington, KY 40506.

This article contains supporting information online at https://www.pnas.org/lookup/suppl/doi:10.1073/pnas.2514344122/-/DCSupplemental.

Published October 27, 2025.

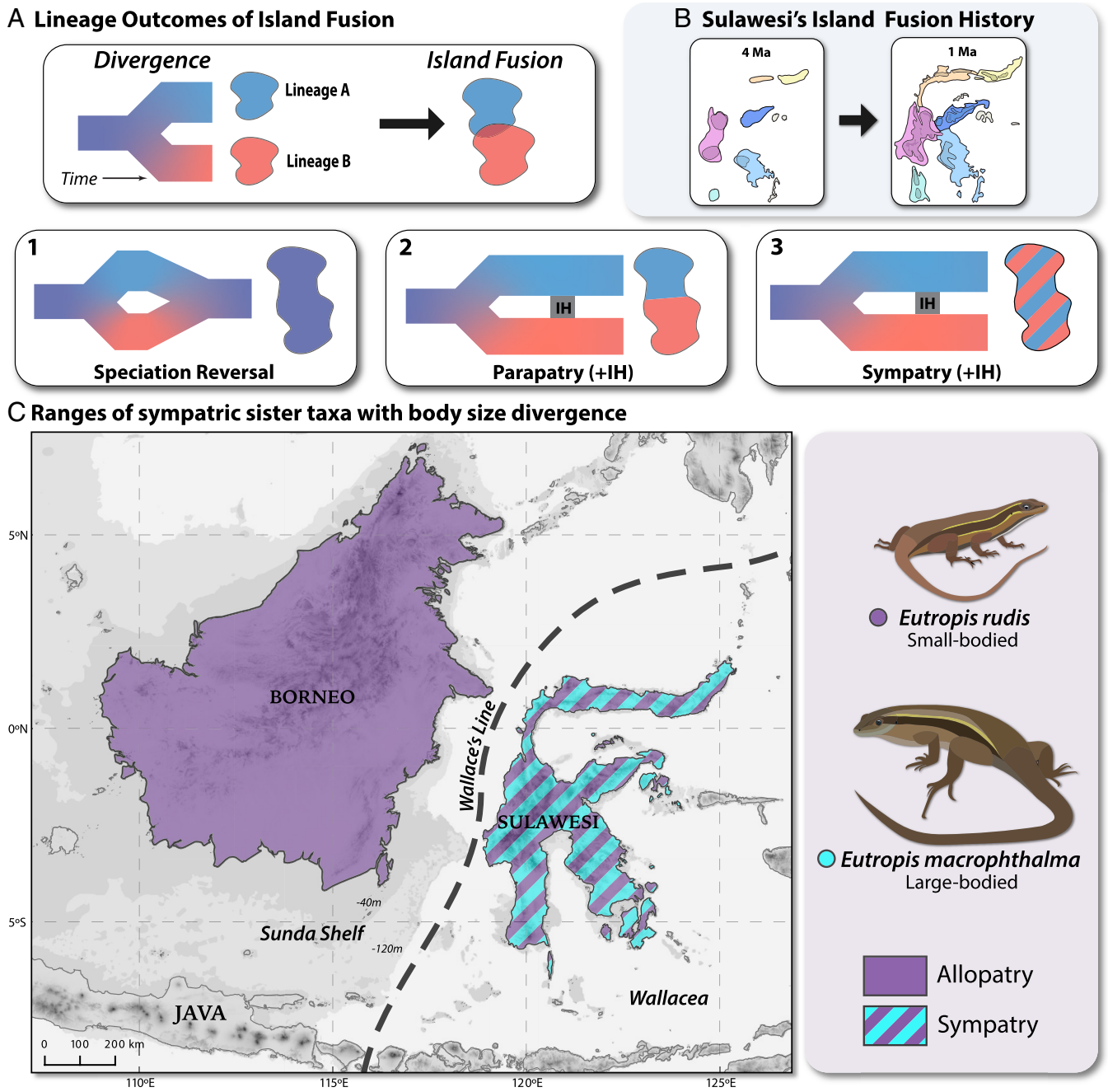

Fig. 1. Illustration of the three possible outcomes of secondary contact during island fusion and overview of study system. (*A*) When islands with isolated, divergent lineages fuse, it provides an opportunity for secondary contact with three possible outcomes and varying degrees of introgressive hybridization (IH). (*A*1) They may experience such substantial IH that speciation reverses and the lineages merge. (*A*2) Lineages may form a stable contact zone and become parapatric with varying degrees of IH. (*A*3) The lineages may have either diverged ecologically in isolation or may experience postcontact character displacement allowing full species sympatry, which also could be coupled with IH. (*B*) Sulawesi has undergone a dynamic paleogeographic history in which six primary paleo-islands fused to form Sulawesi's present configuration. (*C*) The two focal taxa, *Eutropis rudis* and *Eutropis macrophthalma* have a two-fold divergence in body size. They are sympatric on Sulawesi, and *E. rudis* also ranges across Wallace's Line to Borneo.

lineages or through incompatibilities (13–15). Incompatibilities may promote divergent selection when interlineage mating produces unfit hybrids—reinforcement (16). Yet few studies have tested these predictions across multiple lineage pairs with well-understood histories.

A growing body of research has demonstrated that key markers of speciation, such as the strength of reproductive incompatibilities, the probability of reinforcement, and the narrowness of hybrid zones, all increase with genetic divergence (6, 17–20). Extending this framework, theoretical models and empirical observations have identified a sigmoidal divergence threshold or "tipping point" where the outcome of hybridization rapidly switches from speciation reversal to progression with increasing divergence (measured variously as Fst or Dxy, or compared using divergence times which are correlated with genetic divergence) (21–24). However, broad comparative studies often lack precise isolation histories (e.g., 21), and contact zone analyses typically reflect only a single outcome—parapatry (e.g., 19). A more complete understanding of how speciation progresses requires robust, replicated empirical systems that link distinct contact outcomes to known histories of isolation and secondary contact (25).

The rare phenomenon of island fusion—where previously separated islands become land-connected due to movement, uplift, or sea-level shifts—creates an exceptional scenario for studying secondary contact (26, 27). Island archipelagos provide "natural laboratories" to investigate evolution because of their discrete boundaries and strong isolation (28), often showcasing rapid diversification (29). Island fusion can push multiple pairs of related lineages, potentially with different degrees of divergence, into contact within a shared geographic and environmental context, offering a powerful comparative framework.

The Indonesian island of Sulawesi represents such an extraordinary natural experiment. Its peculiar K-shape results from a complex geological history involving the amalgamation of six primary paleo-island fragments (Fig. 1*B*) (30). This fusion process, occurring primarily from 3 to 1 Ma following as much as 25 Ma of isolation (30), profoundly shaped the island's highly endemic fauna with distributions of many taxa reflecting the boundaries of these ancestral paleo-islands (31). This history implies repeated instances where lineages diversified in isolation on separate paleo-islands and were subsequently brought into secondary contact as the landmasses coalesced, resulting in Sulawesi's high species richness and endemicity (12, 32, 33). Sulawesi thus provides a spatially and temporally explicit framework to investigate whether divergence accumulated during isolation dictates the outcome of secondary contact. Both ancient hybridization and arrested speciation have been detected in some taxa on Sulawesi (12, 34, 35), but it remains untested if these are repeated consequences of secondary contact due to island fusion or other processes.

Here, we utilize this replicated paleogeographic framework to investigate the outcomes of secondary contact along the speciation continuum in a small and nearly unstudied radiation of *Eutropis* sun skinks. The focal clade consists of two described taxa, *Eutropis rudis* and *Eutropis macrophthalma*, distributed across Sulawesi and Borneo that exhibit two-fold body-length and five-fold body mass divergence (Fig. 1*C*) (36, 37). They are fully sympatric on Sulawesi occurring in the same microhabitats with overlapping elevational ranges on Sulawesi's mountains (38). Previous genus-wide studies with limited intraspecific sampling have supported them as sister taxa (39, 40), but no range-wide phylogenetic research has investigated whether divergent lineages exist within each. *Eutropis rudis* has a unique distribution spanning Wallace's Line which traces the edge of the Sunda continental shelf (between Borneo and Sulawesi) and is a major biogeographic barrier for many taxa (33).

We studied the evolution of this group using nearly 200 genetic samples and 500 morphological samples collected over decades of field research in Sulawesi and Borneo. We generated a genome-wide and densely geographically sampled dataset and integrated coalescent species delimitation, explicit tests for hybridization, phylogenomic network inference, demographic modeling, and reconstructions of ancestral body size and biogeographic history. We found that sun skinks colonized the Sulawesi paleo-archipelago from the adjacent Sunda Shelf and subsequently diversified across the paleo-islands before experiencing secondary contact driven by island fusion. We leveraged replicated island fusion events on Sulawesi to empirically test whether the outcomes of secondary contact within this radiation—ranging from reversal to parapatry to sympatry associated with phenotypic divergence—are dependent on the evolutionary divergence accumulated during isolation. By resolving the complex reticulate history of this group, we were able to develop a synthetic understanding of their unique evolutionary history that included overwater dispersal to isolated islands, introgressive hybridization (IH) with strikingly different outcomes, and pronounced shifts in body size, providing a unique glimpse into the speciation continuum.

Results

Phylogenomics Reveals a Cryptic Radiation Shaped by Hybridization. Our investigation into the *Eutropis rudis-macrophthalma* clade of sun skinks, previously thought to comprise just two species distinguished by body size, uncovered a more complex history involving cryptic diversification with significant hybridization events. Initial mitochondrial screening revealed deep divergences within the small-bodied taxon, *E. rudis*, hinting at unrecognized lineages across some of Sulawesi's paleo-islands (Fig. 2*A*). Subsequent phylogenomic analyses of 8.6 Mbp of nuclear data, including rapidly evolving long exon capture (RELEC) loci that maximize phylogenetic information content (41), confirmed this cryptic diversity and revealed a complex history of gene flow.

Species delimitation using a multispecies coalescent with migration (MSC + M) model (42) supported a hypothesis of five distinct species originating from a single colonization of Sulawesi (Fig. 2*C*). This includes the large-bodied, Sulawesi-endemic *E. macrophthalma*, and four lineages within the *E. rudis* complex: three previously undescribed, small-bodied endemic species largely restricted to different regions of Sulawesi (ENP: Eastern Northern Peninsula; West Sulawesi: Western Northern Peninsula + Western Central Core; SW + SE + E: Southwest + Southeast + Eastern Peninsulas), and one representing *E. rudis* sensu stricto, now confined to Borneo but nested within the Sulawesi radiation. Genomic differentiation between these lineages was substantial, with Genealogical Discordance Index (GDI) values above 0.7 which usually indicates distinct species (*SI Appendix*, Tables S4 and S6). Only the Borneo and SW + SE + E sister lineages had ambiguous GDI values of 0.56 and 0.41, respectively, yet we still consider these distinct species based on nonoverlapping adult body size and low contemporary gene flow. We will formally diagnose and name these undescribed species in future work, but our species delimitation provides robust operational units for investigating evolutionary processes in this study. See supplementary text for other taxonomic implications.

Reconstructing the precise evolutionary relationships among these five species proved challenging due to three cases of ancient IH. Standard MSC methods which assume strictly bifurcating evolution with discordance driven only by incomplete lineage sorting (ILS), yielded highly supported but conflicting topologies. Specifically, the ENP lineage was consistently misplaced due to "introgression attraction"—its phylogenetic position artifactually shifted toward *E. macrophthalma*, which we later found to be the result of substantial gene flow—rather than reflecting the primary backbone history (Fig. 2*B* and *SI Appendix*, Fig. S8). Furthermore, divergence time estimates under these bifurcating phylogenetic estimates were unreliable, displaying pathological node age compression where distinct divergence events appeared artificially simultaneous (*SI Appendix*, Fig. S8). These artifacts highlight that failing to account for IH can produce positively misleading results, even with large datasets (also see 12).

Explicit tests for introgression confirmed the presence and sources of hybridization. Significant differences in discordant gene tree quartet frequencies across all data types indicated IH involving the ENP lineage (Fig. 3*A* and *SI Appendix*, Fig. S11). Site-based methods (ABBA-BABA and f-branch tests using >1.3 million SNPs) confirmed introgression between *E. macrophthalma* and ENP (Fig. 3*B* and *SI Appendix*, Table S8). They also detected introgression between West Sulawesi and both SW + SE + E and Borneo (or their common ancestor).

Full Bayesian phylogenetic network inference, which explicitly models both ILS and IH and integrates across gene tree uncertainty, recovered a strongly supported network topology. This full

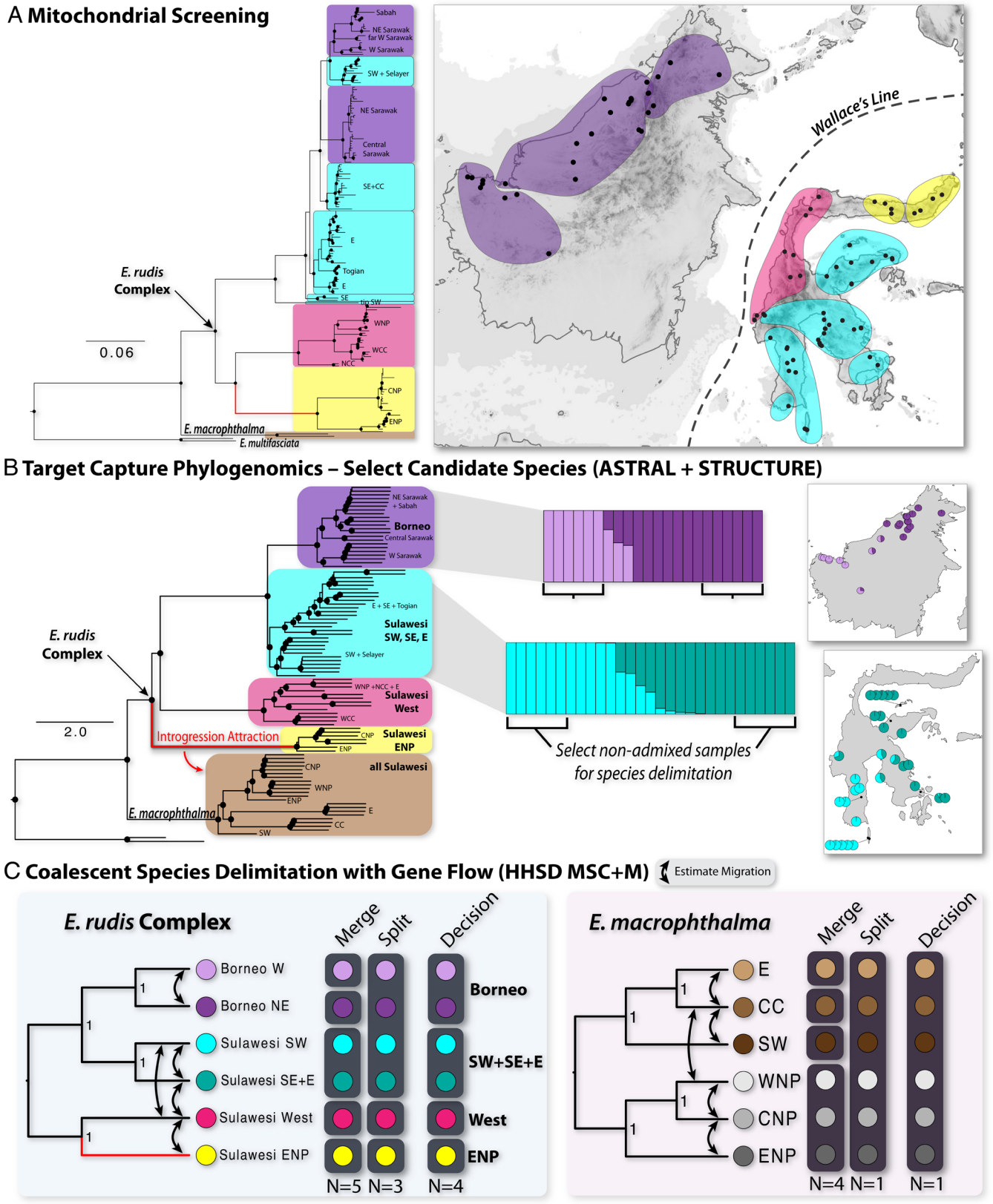

Fig. 2. Overview of the coalescent species delimitation workflow. (*A*) We first conducted mitochondrial screening at high spatial resolution to assess the major clades present in the dataset. We then selected representative samples for target capture phylogenomics. Circles at nodes have ≥70% bootstrap support. (*B*) ASTRAL-HYBRID topology on the combined set of 3,416 loci and population admixture plots for key clades. Circles at nodes have 100% support. This topology was influenced by introgression attraction in which ENP was drawn toward the source of introgression, *E. macrophthalma*. We selected candidate species for coalescent species delimitation based on the combined results of ASTRAL and STRUCTURE. (*C*) We employed Hierarchical Heuristic Species Delimitation (HHSD) using a multispecies coalescent plus migration (MSC + M) model that accounts for gene flow between land-connected candidate species (designated by arrows). We generally followed the conservative split algorithm result (GDI ≥ 0.7) except for the Borneo lineage which is substantially larger than the SW + SE + E lineage. Node labels are posterior probabilities for the separate guide tree estimation. The red branch to ENP highlights the different topologies obtained using strictly bifurcating MSC analyses compared to the other analyses.

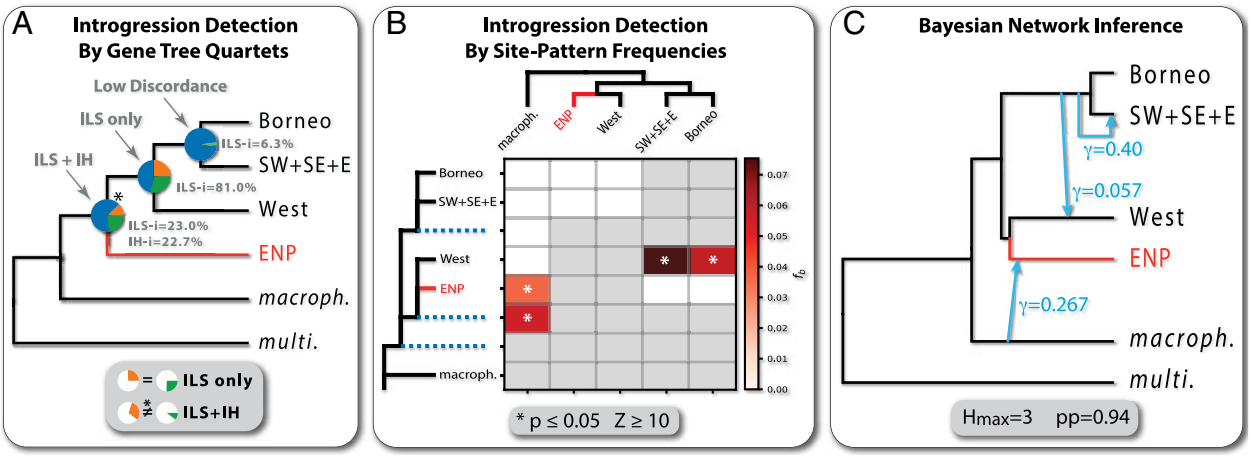

Fig. 3. We detected strong signatures of hybridization between the delimited species. (*A*) Gene tree quartet tests for introgression detected significantly different frequencies of discordant quartets (orange and green proportions) on the node to the ENP lineage. ILS-i and IH-i correspond to the extent of incomplete lineage sorting (0 to 100%) and IH (0 to 50%), respectively. Results for the RELEC data are displayed, but the three other data types had consistent results. (*B*) F-branch test for introgression based on site-pattern frequencies for >1.3 million SNPs. The color of red corresponds to the degree of allele sharing, with asterisks representing significant F-branch statistics. Gray boxes correspond to untested comparisons based on the topology. (*C*) Best-scoring Bayesian network topology based on the RELEC loci with three allowed reticulation events (Hmax) matched the topology at Hmax = 4. The hybrid edge from *E. macrophthalma* into ENP was inferred across all values of Hmax. The network posterior probability (pp) is displayed. In all panels, the red branch to ENP highlights the different topologies obtained using strictly bifurcating vs. network analyses.

likelihood approach is expected to outperform site-based and two-step network inference approaches which may incorrectly specify the direction of introgression and struggle to detect ghost introgression arising from an extinct or unsampled lineage (43). The network with three hybrid edges was best supported even by analyses with larger numbers of allowed reticulations (Fig. 3*C*; *SI Appendix*, Fig. S20). This network had a backbone phylogeny consistent with the mitochondrial data and placed hybrid edges consistent with the introgression detection tests. The first substantial introgression event (γ ≈ 24 to 35%) occurred from *E. macrophthalma* into ENP (Fig. 3 and *SI Appendix*, Fig. S20). The second relatively limited introgression (γ ≈ 5.7%) occurred from the ancestor of SW+SE + E + Borneo into West Sulawesi. A third substantial introgression (γ ≈ 40%) from an unsampled ghost lineage stemming from the same ancestor into SW + SE + E likely corresponded to the initial splitting of now merged lineages (see "Speciation Reversal" section below). Two-step network inference only detected the first of these three introgression events across all four data types (γ ≈ 23.5 to 27.0%). The three-introgression model was validated by Bayes Factor testing in BPP (all BF>150), and no other introgression events between parapatric or sympatric taxa were supported. Demographic modeling under the MSC+I model in BPP estimated the timing of the introgression events between 1 and 3 Ma for all datasets (Fig. 4*A*). This timing aligns remarkably well with the primary period of Sulawesi's paleo-island fusion (~3 to 1 Ma), supporting that island coalescence facilitated secondary contact and hybridization between these previously isolated lineages (Fig. 4*C*). The BPP estimated divergence times between species were consistent with an additional BEAST analysis on the genus-wide supermatrix based on commonly used mitochondrial molecular clock calibrations.

Secondary Contact Outcomes are Associated with Divergence Time. Sulawesi's sun skink radiation, shaped by paleo-island fusion, provides a compelling system to illustrate how the outcomes of secondary contact relate to the degree of prior divergence. The different pairs of lineages pushed into contact represent distinct points along the speciation continuum, and their resulting interactions exhibit the full spectrum of predicted outcomes (Fig. 4 *E* and *F*):

- **Speciation Reversal:** The populations occupying the historically separate Southwest (SW), Southeast (SE), and Eastern (E) paleo-islands are mitochondrially distinct but represent the lowest level of divergence within the *E. rudis* complex prior to secondary contact. Whereas they may have once represented distinct lineages, the genomic data indicate that they now form a single, widespread species (SW + SE + E) exhibiting clinal variation based on STRUCTURE analysis (Fig. 2*B*). While nuclear data display admixture and low GDI of 0.2 for SW and 0.29 for SE+E (near the 0.2 threshold below which a sample set unambiguously represents a single lineage), mitochondrial DNA retains deeper structure corresponding to the ancestral paleo-islands. A single individual with a divergent mitochondrial haplotype at the southernmost tip of the SW peninsula may correspond to the now-merged ghost lineage that contributed about half its alleles (γ ≈ 40%, 95% HPD for ϕ 46 to 59%). Introgression from the ghost lineage occurred around 1.1 to 1.2 Ma, potentially with the fusion of the SW peninsula to the remainder of Sulawesi. This outcome supports the theoretical expectation that insufficient precontact divergence allows gene flow to overwhelm early barriers, leading to the collapse of lineage boundaries. The ENP species also holds a deep mitochondrial break (9 to 12% uncorrected pairwise divergence for the ND2 gene) that is now encapsulated within a more widespread nuclear lineage. This may also correspond to reversed or arrested speciation, but since this does not occur at a modeled paleo-island boundary we did not investigate it in more detail in this study.
- **Parapatry:** Two pairs of lineages that exhibit intermediate levels of divergence developed parapatry after secondary contact, one with limited introgression and the other with no inferred introgression. The older pair, West Sulawesi and SW + SE + E, form a contact zone across the central core and occur in narrow sympatry on the Eastern Peninsula. For this older pair our network analyses and site-pattern tests detected ancient, low-level introgression (γ ≈ 5.7%, 95% HPD for ϕ 2.4 to 8.8%) from the SW + SE + E and Borneo ancestor into West Sulawesi, estimated to have occurred around 2.7 to 3 Ma depending on the analysis, likely with the concordant uplift

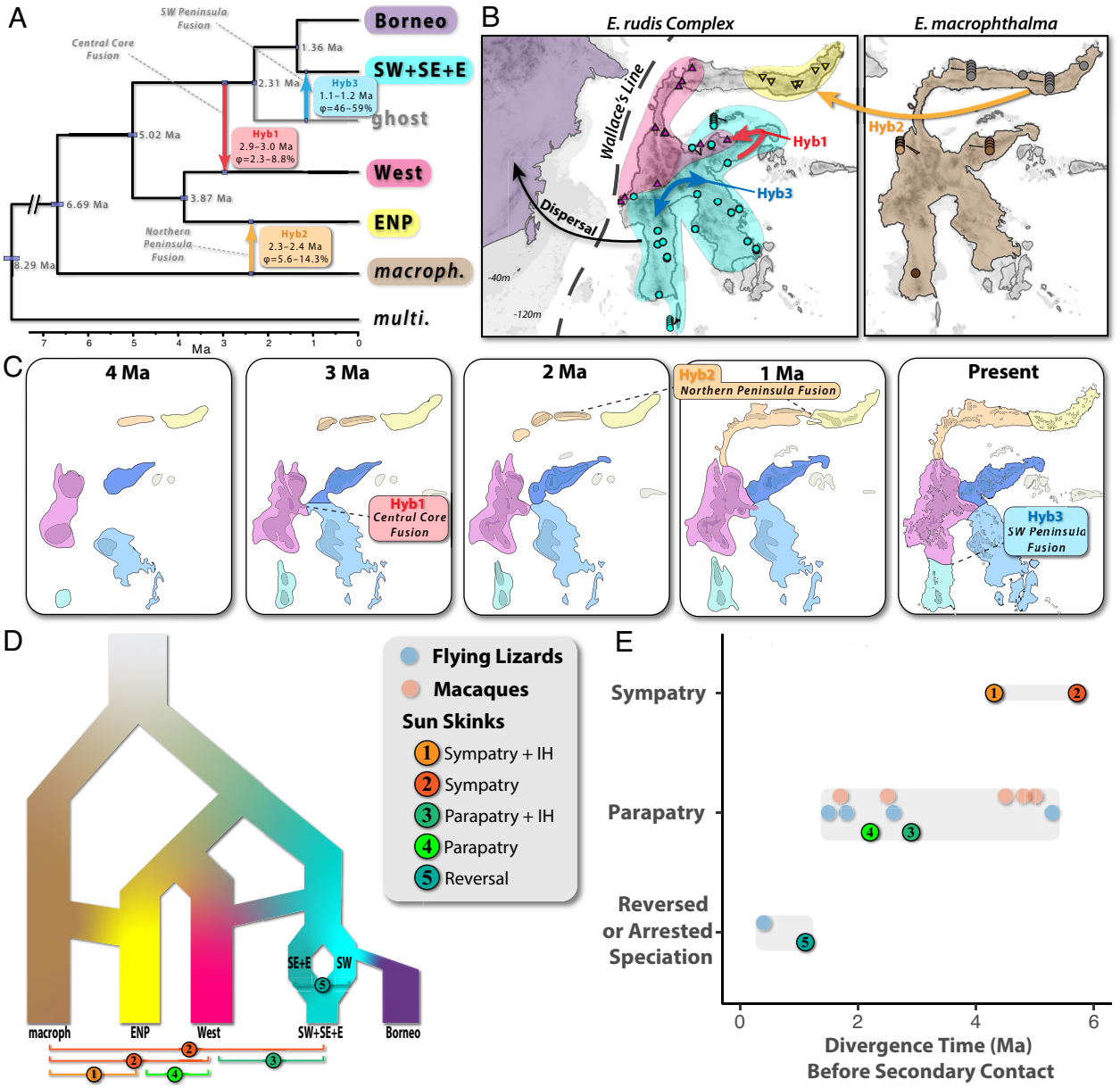

Fig. 4. The estimated timings of introgression events are concordant with secondary contact during the fusion of Sulawesi's paleo-islands and the outcomes are associated with divergence time. (*A*) BPP MSC+I analysis found that the initial divergence of all lineages occurred before paleo-island fusion commenced, and that the timing of introgression events occurred near the time of island fusion. The RELEC dataset BPP analysis is displayed, but other datasets had similar age estimates. Divergence times are written at nodes with bars representing their 95% HPD intervals. For the three introgression events (Hyb1–3), 95% HPD intervals are displayed for introgression times and introgression coefficient. (*B*) Geographic summary of the history of hybridization. In chronological order, the first hybridization (Hyb1) occurred from large-bodied *E. macrophthalma* into ENP most likely on the Northern Peninsula as it fused. Hyb2 from SW + SE + E into West Sulawesi likely occurred on the Eastern Peninsula where there exists limited mitonuclear discordance. Hyb3 occurred from a ghost lineage to form the merged SW + SE + E lineage, likely as the SW peninsula fused. (*C*) Maps displaying the paleo-island history of Sulawesi (adapted from ref. 30), with key island fusion events associated with hybridization labeled. (*D*) Summary of the lineage history of the clade with sympatry, parapatry, and reversal events labeled. (*E*) For sun skinks, flying lizards, and macaques, divergence times before secondary contact form discrete intervals for each lineage process.

of Sulawesi's central land bridge between 4 and 3 Ma according to geological models (30). Estimates of contemporary migration are very low (*SI Appendix*, Table S5), and despite limited mitochondrial capture in the Eastern Peninsula contact zone, there is no signature of nuclear admixture (*SI Appendix*, Fig. S9). Conversely, the younger pair, ENP and West Sulawesi, must form a contact zone in the small sampling gap on the Northern Peninsula but do not maintain any lasting signal of introgression or gene flow. The contact zone probably occurs near the Gorontalo Fault which is a paleo-island and species boundary for several taxa (12). This suggests that, for both pairs, reproductive incompatibilities were strong enough by the time of contact to prevent extensive introgression and establish stable parapatric boundaries. Future sampling of these putative hybrid zones will provide insights into the degree of reproductive isolation and additional evidence for the taxonomic status of these lineages.

- **Sympatry and Associated Body Size Divergence:** The three most divergent secondary contact pairs occur in sympatry, each involving the large-bodied *E. macrophthalma* and one of the three parapatric small-bodied *E. rudis* complex species. The introgression from *E. macrophthalma* into ENP was inferred to be substantial ($\gamma \approx 24$ to 35%, 95% HPD for ϕ 5.6 to 14.3%) and caused major pathological issues for MSC analyses. This

hybridization was estimated to occur around 1.7 to 2.4 Ma and is likely associated with the rapid uplift of the northern peninsula by 2 Ma and eventual fusion by at least 1 Ma (30). Despite ancient hybridization between *E. macrophthalma* and ENP, contemporary gene flow appears absent, indicating the evolution of robust reproductive isolation. This sympatry is coupled with extreme body size divergence (Fig. 5). *E. macrophthalma* adults are on average >50 mm longer in snout–vent length (SVL) (mean 124.4 mm) than the sympatric *E. rudis* complex species (mean=71.2 to 73.1 mm; $p < 0.001$) and ~5 times the body mass (mean = 49.0 g versus 10.6 to 11.4 g adult mass; $p < 0.001$). Genus-wide bifurcating (Fig. 5) and network (*SI Appendix*, Fig. S25) ancestral character reconstructions consistently estimated an intermediately sized common ancestor, implying body size divergence occurred after lineage divergence.

Discussion

Outcomes of Secondary Contact. Collectively, the distinct outcomes of secondary contact—speciation reversal, parapatry, and sympatry—observed within a single radiation and correlated with divergence times estimated from robust genomic data provide empirical validation for the concept of divergence-dependent tipping points along the speciation continuum. Crown divergences of other Sulawesi exemplar radiations of macaques and flying lizards (6.4 and 6.3 Ma) (12, 44) began at virtually the same estimated time as for sun skinks (6.7 Ma), but these radiations primarily established parapatry at paleo-island boundaries whereas the sun skinks display all three outcomes. Flying lizards do display three cases of lineage merger despite retention of deep mitochondrial structure, but two of these cases do not occur specifically at paleo-island boundaries (within the island's Central Core), and they therefore could be the result of different isolating forces within the designated paleo-islands (12).

To compare the speciation process across taxa, researchers often use metrics that quantify average pairwise genomic divergence to provide a snapshot of the current state of differentiation and its association with the present degree of reproductive isolation (e.g., extent of ongoing gene flow). Alternatively, divergence times, which are correlated with genetic divergence, can be used to estimate the degree of divergence at a specific point in the past, such as at the time of secondary contact. Here, we focus on divergence times to compare the progression of speciation across taxa, since our historical biogeographic framework leverages outcomes of ancient geographic events leading to contact following strong isolation. Because substitution rates vary among taxa, divergence times are not inherently reflective of the biological processes underlying speciation but instead provide a correlated timescale linking lineage history to secondary contact outcomes. By comparing the timings of secondary contact with those of Sulawesi macaques and flying lizards we found that the cases of reversal and sympatry in sun skinks occur at the youngest and oldest divergence times, respectively, consistent with thresholds for speciation outcomes (Fig. 4*E*). This first tipping point between speciation reversal and progression (~1.2 Ma divergence time) aligns with studies in other taxa that have identified a sharp, sigmoidal relationship between genetic divergence and hybridization outcomes—where small increases in divergence across a narrow set of intermediate values initiates merger vs. progression (21–23). This threshold should not be interpreted as deterministic or as a universal rule

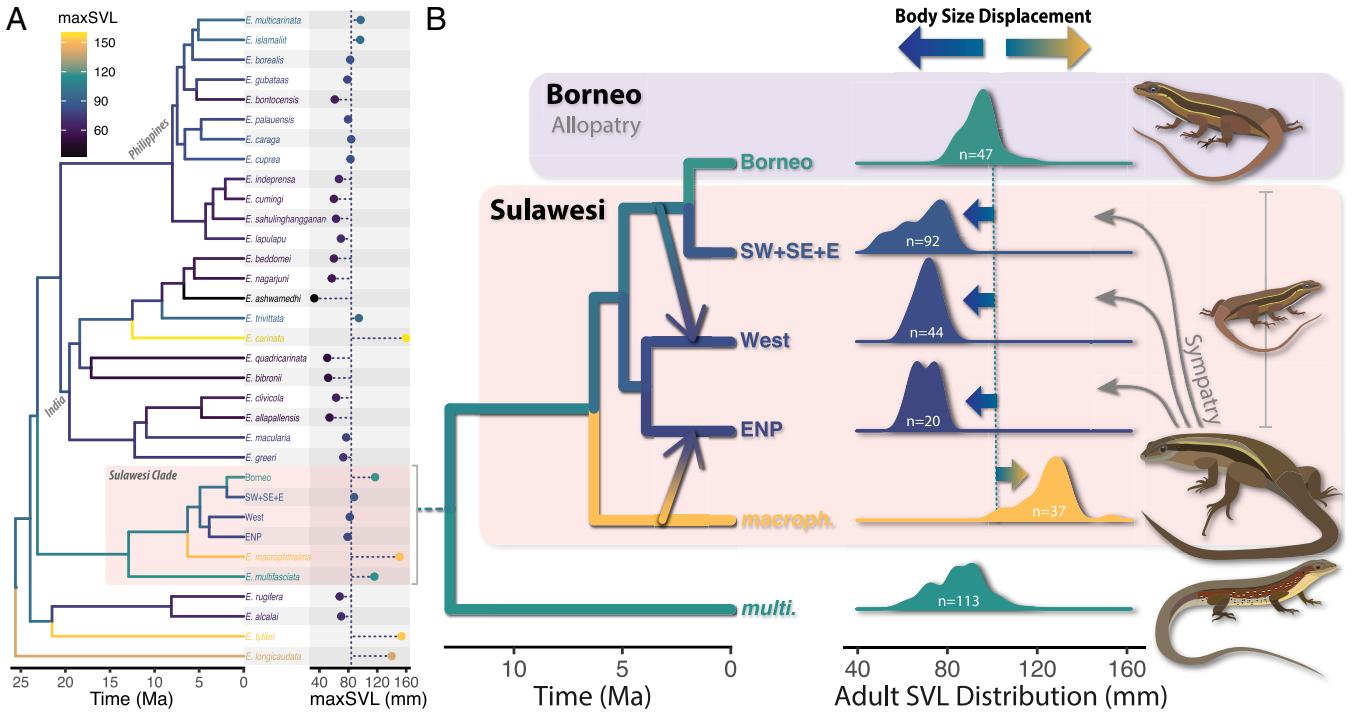

Fig. 5. Body size evolution across the genus *Eutropis* and the focal Sulawesi clade. (*A*) The ancestral character estimation of maximum snout–vent length (SVL) across the genus indicates that large body size (≥140 mm) has only evolved in four species and the Sulawesi clade displays relatively wide variation across recent divergence. The average maximum SVL is indicated by the vertical dashed lines with the focal clade highlighted. (*B*) Magnified view of body size evolution in the Sulawesi clade with corresponding SVL distributions from our field collections. An intermediate sized ancestor is estimated to have diverged into the small and large-bodied lineages on Sulawesi. The intermediate-sized, allopatric Borneo lineage could have dispersed to that island before size displacement on Sulawesi occurred (see *Discussion* for details). The two inferred hybridization edges between extant lineages are displayed on the tree, but colors correspond to the same bifurcating genus-wide ancestral reconstruction on the left (see *SI Appendix*, Fig. S25 for network analysis). The three small-bodied Sulawesi lineages were not significantly different in size, but all other SVL comparisons were significant ($P < <0.01$). Displacement arrows illustrate deviations from the estimated ancestral maximum SVL of the highlighted species (vertical dashed line).

that may be used to, for example, delimit species, as any given empirical system may exhibit stochastic variation or group-specific idiosyncrasies that impact the shape of this relationship. Instead, our findings validate and extend a model for the progression of speciation that has been supported across broad taxonomic groups.

Our results also hint at a possible second threshold from parapatry to sympatry driven putatively by reinforcement (see *Discussion* below). However, more pairs of reproductively displaced sympatric species are needed to establish the shape of this curve and generality of this relationship across different groups. Nevertheless, our detailed findings within Sulawesi's sun skinks provide a deeply resolved case study that lays foundational empirical groundwork for understanding these divergence-dependent transitions. We encourage future research investigating the sun skink contact zones in more detail and exploring secondary contact outcomes in other radiations on Sulawesi and elsewhere shaped by island fusion events. Lineage pairs in other Sulawesi radiations with substantial sympatry, such as sphenomorphine skinks and *Limnonectes* frogs, offer promising systems to test whether these outcomes are more generalizable across taxa (38). If a divergence threshold between parapatry and sympatry exists, our data suggest it may not be as conserved across taxa as the first tipping point between reversal and progression. Several macaque and flying lizard pairs were pushed into secondary contact at a similar time as the oldest *E. macrophthalma* pairs (4.3 to 5.3 Ma) yet became parapatric rather than sympatric (Fig. 4*E*). Experimental speciation research has found that early reproductive isolation is often initiated by adaptation to divergent environments before secondary contact (45). Sympatry may then be more achievable by taxa with greater plasticity or adaptive capacity for phenotypic divergence of reproductive traits before secondary contact, at which time reinforcement or divergent selection can promote further reproductive isolation. This may explain differences in these "rules" across different taxonomic groups and why sun skinks achieved sympatry with substantial body size divergence.

Reproductive Versus Ecological Character Displacement. Extreme size divergence following secondary contact of close relatives strongly implicates character displacement driving body size divergence, but distinguishing the relative roles of reproductive and ecological character displacement can be difficult. Reproductive character displacement requires that the selected trait impacts the probability of mating (16). No mating experiments have yet been conducted in this system, but the nearly two-fold body length and five-fold mass difference between *E. macrophthalma* and each of the three sympatric small-bodied lineages is more than twice what is needed to produce mechanical prezygotic reproductive incompatibility in other similarly sized scincid lizards with the same mating posture (46, 47). Selection then may have favored size divergence to prevent costly, maladaptive hybridization due to incompatibilities after secondary contact (16). As the now larger *E. macrophthalma* lineage expanded across the fusing Sulawesi, it could have imposed a similar selective pressure on other *E. rudis* complex lineages it encountered, driving them toward smaller sizes without leaving behind a signal of hybridization with those specific lineages. While ecological divergence and competition with other species on Sulawesi cannot be excluded from contributing to body size divergence (48), the reduced lizard fauna on Sulawesi (compared to Borneo) has no other large, terrestrial, heliothermic lizard competitors that we expect to compete with this group. The combination of ancient introgression and putative body-sized-based mechanical reproductive incompatibility provide compelling support for reproductive interference as at least a partial driver of this dramatic phenotypic divergence. Specifically, *E. macrophthalma* and ENP must have been reproductively compatible at the initiation of secondary contact, as evidenced by substantial ancient hybridization, but subsequently evolved robust reproductive isolation given their current sympatric occurrence without contemporary gene flow. This trajectory, coupled with the extreme body size divergence that likely impedes interspecific mating, supports a scenario of character displacement facilitating sympatry. This is consistent with research showing that the probability of reinforcement increases with divergence (6, 18), and that sympatric speciation is most often aided by gene flow (49). It is remarkable that this sympatry with complete reproductive isolation could occur after such substantial introgression of up to 20 to 35% of alleles, though this is not unprecedented (50, 51).

A Reverse Crossing of Wallace's Line. Beyond Sulawesi, our phylogenomic analyses firmly indicate that the *E. rudis* lineage on Borneo is derived from within the Sulawesi radiation, and the mitochondrial data support it as originating via overwater dispersal from the SW Peninsula or southern Central Core (Fig. 4*A*). The genus-wide biogeographic model confirmed that this colonization occurred from Sulawesi to Borneo (*SI Appendix*, Fig. S21)—a reverse crossing of the famous Wallace's Line (52). Wallace's Line represents one of the planet's most dramatic faunal boundaries, reflecting the deep-water separation between the Sunda continental shelf (Borneo) and Sulawesi (33), and our results indicate that sun skinks completed this journey at least twice. This finding challenges the assumption of unidirectional dispersal from Sundaland as a source into Wallacea (33), consistent with recent research that found Wallace's Line to be permeable at early stages of divergence (34). Indeed, we found two narrowly divergent mitochondrial clades on Borneo, one of which was more closely related to SW Sulawesi (Fig. 2*A*). This suggests a possible third crossing, perhaps back to Sulawesi soon after Borneo was established.

Body Size Evolution Across Wallace's Line. The body size evolution of this clade involves not only the nearly two-fold sympatric body length divergence on Sulawesi but also the intermediate size of the allopatric Borneo species. Borneo *E. rudis* exhibits an intermediate SVL nearly precisely between the size of the small Sulawesi sister lineage (SW + SE + E) and the large *E. macrophthalma* (Fig. 5). Intriguingly, this intermediate size is similar to the reconstructed ancestral SVL for the Sulawesi group. Several hypotheses could explain this pattern. The Borneo lineage might have experienced ecological character displacement upon colonizing the more diverse Sundaic lizard community and evolved larger body size from a small Sulawesi ancestor (16). For example, the small-bodied congener, *Eutropis rugifera*, is widespread across Borneo (53) and may exert competitive pressure favoring body size divergence. Alternatively, it could represent a release from the character displacement pressure exerted by *E. macrophthalma* on Sulawesi and a shifting optimum in allopatry (54). This is not supported by patterns on Sulawesi's satellite islands, such as Selayer and the Togians, where *E. macrophthalma* has not yet been recorded and the SW + SE + E species is not noticeably different in size. A third compelling possibility relates to dispersal timing: if the dispersal to Borneo (ranging from 1.3 to 1.8 Ma across analyses) occurred before character displacement drove extreme size divergence in the source population on Sulawesi (potentially initiated by hybridization between *E. macrophthalma* and ENP around 2.3 to 2.6 Ma on the Northern Peninsula but perhaps taking time to propagate to SW Sulawesi), then the Borneo population might

simply retain the ancestral, intermediate phenotype. This is supported by the divergence time of the *E. macrophthalma* SW Peninsula population near the Borneo divergence time (1.4 to 1.5 Ma; *SI Appendix*, Table S7), as well as the patterns of introgression, as *E. macrophthalma* most likely hybridized with ENP and diverged in size in that location before it encountered the other species with which it did not hybridize. Despite this moderate support for the hypothesis that Borneo dispersal occurred before size displacement, these alternative scenarios highlight the difficulty of confidently differentiating the large array of ecoevolutionary forces, such as community dynamics and reproductive interference, that shape phenotypic evolution (55).

Biogeographic Synthesis. The biogeographic history of this group has been partially obscured by range expansions, displacement, and gene flow, but key aspects are still clearly discernable. The ancestral area estimates from the clade-specific biogeographic analysis were ambiguous for key internal nodes (*SI Appendix*, Fig. S22), largely due to the widespread distributions of SW + SE + E and *E. macrophthalma,* which each span four to all six paleo-islands, and the relatively small species tree. Nonetheless, the tree topology and present-day distributions provide clues to the biogeographic history. The ENP lineage almost certainly originated via overwater dispersal to the ENP paleo-island prior to its fusion with the rest of the Northern Peninsula. At that time, the SW, SE, and E paleo-islands were likely occupied by now-joined SW + SE + E lineages. This is further evidenced by the remaining mitochondrial structure within this species. The placement of the West Sulawesi and *E. macrophthalma* lineages suggests they occupied the Central Core (CC) and WNP, but their precise paleo-island origins remain unclear.

If *E. macrophthalma* was historically isolated on the WNP, this might explain the substantial IH with the ENP species during uplift of the NP but not with the other *E. rudis* complex lineages. That first hybridization event may have triggered reproductive character displacement, potentially precluding future hybridization with other sympatric taxa as *E. macrophthalma* expanded its range. Conversely, if the West Sulawesi species was restricted to WNP, its hybridization with SW + SE + E would not have occurred until connection of the NP to the CC enabled gene flow. Alternatively, each of the lineages could have been isolated on smaller paleo-island components of the uplifting Northern Peninsula. The timing of introgression between West Sulawesi and SW + SE + E (2.7 to 3.0 Ma), coinciding with the uplift of the central land bridge, as well as the hybridization between *E. macrophthalma* with ENP, together provide limited support for the first scenario. For hybridization to occur at 3 Ma, the West Sulawesi lineage must have been present on the Central Core, and since *E. macrophthalma* only hybridized with ENP, it was likely the first lineage it encountered—probably within or near ENP's restricted range. In any case, the sequence of paleo-island fusions between 3 and 1 Ma aligns with the timing of the associated hybridization events (3.0 and 2.4 Ma) inferred from demographic modeling. The crown age of all the *E. macrophthalma* subpopulations ~1.9 Ma (*SI Appendix*, Table S7) is similar to the inferred timing of ancient hybridization in flying lizards at 1.85 Ma (12), which could also have been associated with the fusion of the NP with the CC.

Reversed Versus Arrested Speciation. The final hybridization joined the SW + SE + E lineages and occurred from an unsampled ghost lineage possibly representing a recently diverged population on the SW peninsula—the last paleo-island to fuse with mainland Sulawesi. While the nuclear genomes of these lineages merged, the original SW mitochondrial lineage appears largely displaced. Only one individual at the peninsula's southern tip retains a likely remnant of the ancestral SW mitochondria, suggesting contrasting outcomes for nuclear and mitochondrial genomes. As the paleo-islands fused, the mitochondrial lineage from the southern central core may have spread south into the SW peninsula replacing the SW mitochondria as the nuclear genomes became admixed. This differs from flying lizards, where a deep mitochondrial break occurs within a peninsula despite what appears to be a near-complete nuclear merger—a case of "arrested speciation" since the mitochondria will continue to diverge and could result in incompatibilities that eventually complete speciation (12). In contrast, sun skinks display what we consider speciation reversal or lineage fusion with an ongoing genomic merger and mitochondrial displacement, leaving no apparent reproductive barriers. This contrast showcases how similar geographic events can yield fundamentally different evolutionary outcomes and how the merging of lineages can obscure evolutionary history. That such processes are actively unfolding on Sulawesi today underscores the island's value as a natural laboratory for studying speciation in action.

Methodological Considerations in Reticulate Evolution. This study also provides valuable insights into the challenges and opportunities of phylogenomic inference in the presence of hybridization. The failure of standard MSC analyses serves as a warning against relying solely on bifurcating models to infer backbone relationships, even when extensive genomic data recover strong statistical support. Explicitly testing for and generating phylogenetic networks are critical steps for accurate evolutionary inference. The performance of network inference methods can also be data dependent (see supplementary text for details). Widely used two-step (summary) maximum pseudolikelihood network inference only detected the substantial introgression from *E. macrophthalma* into ENP and was sensitive to data type. In contrast, one-step Bayesian network inference, despite being computationally intensive and requiring dataset reduction, provided robust results and inferred additional reticulations that matched other analyses. Our results suggest that loci maximizing phylogenetic information content to minimize gene tree estimation error and reduce the number of loci (e.g., RELEC, 41) may be particularly valuable for network inference.

Conclusions. The unique paleogeographic history of Sulawesi, marked by the amalgamation of an ancient archipelago into a single island, created an exceptional natural experiment for studying speciation. Our integrated analyses support theory that the outcomes of secondary contact—ranging from speciation reversal, to the formation of stable hybrid zones, to sympatric coexistence mediated by putative reproductive character displacement—are dictated by the degree of evolutionary divergence accumulated in isolation. Furthermore, our findings highlight the permeability of major biogeographic barriers like Wallace's Line and the complex interplay of ecoevolutionary forces that shape phenotypes such as body size. Methodologically, our work underscores the importance of explicitly accounting for reticulate evolution to avoid erroneous conclusions when studying diversification history. By integrating paleogeography with genomics, these clear instances of secondary contact in Sulawesi's sun skink radiation shed light on the fundamental evolutionary processes generating the planet's biodiversity.

Materials and Methods

Mitochondrial Screening. We screened 191 samples of *E. rudis* for a single mitochondrial gene (ND2) using typical Sanger sequencing methods to develop a preliminary understanding of the major clades and to select samples spanning genetic diversity for target capture phylogenomics. We estimated a maximum likelihood tree using IQTREE v2.1.1 (56) with automatic model selection and partition merging for each of the three codon positions (57).

Sequence Capture. We generated phylogenomic data using target capture of thousands of nuclear loci (8.6 Mbp total) for 93 individuals spanning the clade, plus 2 outgroup samples of *E. multifasciata*. We prepared genomic Illumina libraries and captured target sequences using 82,728,120 custom 120 bp probes. The probeset included rapidly evolving long exons (RELEC, 41), top performing ultraconserved elements (58), and additional filtered sets of exons and their flanking introns from phylogenetic studies on other skinks (59–61). RELEC loci are the centerpiece of our dataset as they maximize per-locus phylogenetic information content while retaining orthology and alignability. We processed raw sequence data using the FrogCap pipeline (62) to assemble loci, call SNPs, and generate alignments. We divided the data into four groups of filtered datasets: 1) 215 RELEC exons; 2) 970 UCEs filtered to include top performing loci; 3) 702 PhyloExons filtered to the top performing loci from previous skink phylogenomic studies; and 4) 1529 introns (concatenated from each gene). See *SI Appendix*, Table S3 and Fig. S2 for dataset attribute comparison.

Summary MSC Analyses. We first built a summary MSC tree on the phylogenomic data to assess the major clades present in the data and compare to the mitochondrial tree. We estimated gene trees using RAxML v8.2.12 (63) under the GTRGAMMA model with 100 bootstrap replicates each. We summarized the gene trees using ASTRAL-HYBRID (64) which weights trees based on branch support on each of the four datasets separately and the combined set.

Population Structure and Assessment of Candidate Species. To assess levels of admixture and establish candidate species for coalescent species delimitation, we ran iterative population structure analyses using STRUCTURE v2.3.4 (65). We first ran these on the entire focal clade then iteratively on each designated population. Most analyses had between 2500 and 4000 SNPs (one biallelic SNP per locus), except the smallest dataset for the ENP clade with 1299 SNPs. We jointly used the results of STRUCTURE and ASTRAL to select candidate species, selecting six nonadmixed samples per candidate population for coalescent species delimitation.

Species Delimitation. We conducted multispecies coalescent species delimitation using the Hierarchical Heuristic Species Delimitation (HHSD) v1.0.0 algorithm (42) under the MSC+M model (66, 67) on the RELEC dataset. HHSD accounts for migration between specified populations, providing a robust assessment of the genetic distinctiveness of candidate species (68). HHSD uses iterative runs of the program BPP on sequence alignments to calculate the genomic discordance index (GDI) which is used to either split or merge species from a guide tree at empirically derived thresholds [split: GDI $\geq$ 0.7, clearly distinct; merge: GDI $\geq$ 0.2, ambiguously distinct; (69)]. We ran HHSD separately for *E. macrophthalma* and the *E. rudis* complex given the patterns of broad sympatry. We used a guide tree estimated by BPP A01 species tree inference on each clade separately (that matched the subsequent network backbone topology). We estimated migration rates in both directions between adjacent land-connected candidate species. We selected the more conservative split results in all but one case (Borneo) due to substantial body size divergence.

Introgression Detection by Gene Tree Quartets. We used the program Phytop (70) to detect signatures of introgression by assessing differences in the frequencies of discordant gene tree quartets at each node in the ASTRAL tree. Under ILS, the proportion of the two discordant quartets should be equal whereas IH will skew this ratio. The ILS index (ILS-i, 0 to 100%) estimates the degree of ILS at the node, and the IH index (IH-i, 0 to 50%) is the inheritance proportion. In ASTRAL, we mapped individuals to species using the delimitation result and ran Phytop separately on each of the four datasets.

Introgression Detection by Site-Pattern Frequencies. The ABBA-BABA test and associated F-branch test detect introgression by assessing whether there is an excess of shared alleles beyond expectations of ILS. We used the Dtrios command in the package Dsuite (71) to estimate Patterson's D statistic and F4 admixture ratios, and used the mitochondrial and Bayesian network backbone topology as the guide tree for the F-branch test. We used all 1,318,846 biallelic SNPs across all loci.

Phylogenomic Network Inference. We performed two-step (summary) maximum pseudolikelihood network inference on all four data types and one-step Bayesian network inference on the RELEC data only due to computational limits. Fully parameterized Bayesian phylogenetic inference methods that coestimate gene trees and species trees directly from the sequence data are considered more robust than two-step methods, but they are computationally intensive. Two-step network inference is relatively fast but uses separately estimated gene trees which can create biases and limitations. We employed SNaQ in PhyloNetworks (72) and InferNetwork_MPL in PhyloNet (73) for two-step pseudolikelihood inference using the RAxML gene trees increasing the maximum number of allowed hybridization edges (Hmax) from 0 to 5. We employed MCMC_SEQ in PhyloNet (73) for one-step Bayesian inference, pruning our dataset to 2 individuals per species, with Hmax from 1 to 4. Only the RELEC dataset converged.

Bayesian Test for Introgression. We validated the PhyloNet_MCMCseq model with three introgression events by approximating the Bayes Factor (BF) on the phi parameters using the Savage–Dickey density ratio (74) using BPP v4.8.0 (75). We used the RELEC dataset for testing with a threshold of 0.01. We tested the inferred three introgression event model, and after finding all introgression events to be strongly supported, we tested introgression events on top of this base model in either direction between all sympatric and parapatric lineages. No other introgression events were supported by BF.

Demographic Analyses. We implemented demographic MSC+I analyses in BPP to estimate divergence times and population sizes on the validated three-introgression network topology. We ran BPP separately on each of the four datasets using six individuals per species and reduced the larger datasets to a random 500 loci to facilitate convergence. We converted coalescence times to divergence times by assuming a mutation rate of 1×10^{-9} substitutions per site per lineage per year, a common conversion in lizards (76) that is consistent with germ-line mutation rates across squamates (77).

Biogeography and Body Size Evolution. We built a genus-wide, species-level supermatrix phylogeny to reconstruct the biogeographic history and evolution of body size of the Sulawesi clade within the context of the entire genus. We used SuperCRUNCH (78) to generate an alignment from GenBank of 3 mitochondrial and 17 nuclear genes containing 32 of the 48 presently described species and integrated representative mitochondrial and target capture data from each of our delimited species. We estimated divergence times with BEAST v2.7.7 (79) using a molecular calibration on each mitochondrial gene, and secondary calibrations both on the root based on a subfamily-wide study (80), and on internal nodes of the Sulawesi clade based on our demographic modeling.

We modeled the biogeographic history using BioGeoBEARS v1.1.3 (81) specifying five geographic regions for the genus-wide analysis corresponding to major Southeast Asian biogeographic regions (Sulawesi as one region). We also ran a time-stratified analysis across the focal clade with separate geographic regions for each Sulawesi paleo-island, but there was insufficient signal in this reduced species tree to strongly support most ancestral areas.

We modeled the evolution of body size across the genus to estimate the ancestral size of the *rudis–macrophthalma* ancestor before body size divergence. We used the maximum SVL of described species primarily from Squambase v1.0 (82) and gathered adult body size data for the focal clade from our field collections. We ran two separate ancestral character estimation analyses on these data modeling state changes using Brownian motion, one on the bifurcating topology using phytools v.2.3 (83) and one on the network topology using PhyloTraits (84) by manually joining the two nonghost hybrid edges. We compared the adult size distributions in the focal clade with ANOVA and Tukey's test.

Data, Materials, and Software Availability. Data files are available on Zenodo (85). Raw nuclear sequence data are deposited on the NCBI SRA database (86). Mitochondrial sequence data are deposited on the NCBI nucleotide database (*SI Appendix*, Table S1).

ACKNOWLEDGMENTS. For fieldwork we thank Anang Achmadi, Mohammad Irham, Pungki Lupiyaningdya, Tri Haryoko, Tri Wahyu Laksono, Dede Avandi, Suparno, Hadi, Umilaela Arifin, Jarot Arizona, David Bickford, Alexander Stubbs, Sean Reilly, Luke Bloch, Fahri, Boy, Safir, Donny Bosco, Frederick Chain, Tom Devitt, Ari Ekapratama, Rosita Elianur, C.J. Hayden, Mistar Kamsi, Ruud de Lang, Rafe Brown, Adam Leaché, Mumpuni, Gilang Ramadhan, Ferdi Rangkuti, Heidi Rockney, Abdul Rosyid, Dan Scantlebury, Iqbal Setiadi, Ted Townsend, Yong Min Pui, Paiz Dlafi, Byezurah Malik, Samuel Shonleben, Ian Brennan, Izneil Nashriq, Jerry Wong, Franey Chong, Aderina Dukit, and countless other local people who welcomed us onto their land and into their homes. We thank Carol Spencer and her curatorial team for accessioning of specimens at the Museum of Vertebrate Zoology, and Lydia Smith, Kayla Walzer, Laura Wang, and Selene Arellano for assistance with lab work. We thank the McGuire, Wang, and Bauer-Jackman Lab Groups, as well as the Bonnie Brain Trust for feedback on results and earlier versions of this manuscript. We also thank two anonymous reviewers for their critical peer-reviews of the manuscript. Fieldwork on Sulawesi was conducted under permits granted by the Indonesian Institute of Sciences (LIPI) and RISTEKDIKTI (now BRIN). Fieldwork in Sarawak was conducted under permits issued by the Sarawak Forestry Corporation (NCCD.907.4.4(Jld.11)-68). Fieldwork in named anchornamed anchor Sabah was conducted under permits issued by the Sabah Biodiversity Council [Access permits: B.R.K.: named anchor JKM/ MBS.1000-2/2 JLD.19(33), E.S.H.Q.: JKM/ MBS.1000-2/2 JLD.19(34); Export permit: JKM/ MBS.1000-2/3 JLD.5(82)], the Board of Trustees of Sabah Parks (TTS 100-6/2 Jld. 33), and the Sabah Forestry Department [JPHTN/PSH 100-14/18/2/JLD.22(36), JPHTN/KK 700-2/1/JILID.7(39)]. Animal study protocols were approved by the Institutional Animal Care and Use Committees of the University of California Berkeley and Villanova University.

Author affiliations: [a]Museum of Vertebrate Zoology and Department of Integrative Biology, University of California, Berkeley, CA 94720; [b]Department of Biology and Center for Biodiversity and Ecosystem Stewardship, Villanova University, Villanova, PA 19085; [c]Laboratory of Herpetology, Museum Zoologicum Bogoriense, Research Center for Biosystematics and Evolution, National Research and Innovation Agency, Cibinong, Bogor 16911, Indonesia; [d]Research Center for Biota Systems, National Research and Innovation Agency, Cibinong, Bogor 16911, Indonesia; [e]School of Life Sciences and Technology, Bandung Institute of Technology, Bandung 40132, Indonesia; [f]Basic Sciences Commission, Indonesian Academy of Sciences, Jakarta 10110, Indonesia; [g]Institute of Biodiversity and Environmental Conservation, Universiti Malaysia Sarawak, Kota Samarahan, Sarawak 94300, Malaysia; [h]Wildlife Biology Program, Division of Biological Sciences, University of Montana, Missoula, MT 59812; [i]Sabah Landscape Programme, World Wildlife Fund Malaysia, Kota Kinabalu, Sabah 88000, Malaysia; [j]Institute for Tropical Biology and Conservation, Universiti Malaysia Sabah, Jalan UMS, Kota Kinabalu, Sabah 88400, Malaysia; and [k]Lee Kong Chian Natural History Museum, National University of Singapore, Singapore 117377, Singapore

Author contributions: B.R.K., J.H.F., A.H., A.R., E.A., D.T.I., I.D., A.S., E.S.H.Q., T.R.J., A.M.B., and J.A.M. designed research; B.R.K., J.H.F., A.H., A.R., E.A., D.T.I., I.D., A.S., E.S.H.Q., T.R.J., A.M.B., and J.A.M. performed research; B.R.K., J.H.F., A.H., A.R., E.A., D.T.I., I.D., A.S., E.S.H.Q., T.R.J., A.M.B., and J.A.M. contributed new reagents/analytic tools; B.R.K. and J.A.M. analyzed data; B.R.K., T.R.J., A.M.B., and J.A.M. secured Funding; and B.R.K. and J.A.M. wrote the paper.

The authors declare no competing interest.

1. J. A. Coyne, H. A. Orr, *Speciation* (Sinauer Associates, Oxford University Press, 2004).
2. R. Abbott *et al.*, Hybridization and speciation. *J. Evol. Biol.* **26**, 229–246 (2013).
3. S. Gavrilets, Perspective: Models of speciation – What have we learned in 40 years? *Evolution (N.Y.)* **57**, 2197–2215 (2003).
4. J. V. Peñalba *et al.*, The role of hybridization in species formation and persistence. *Cold Spring Harb. Perspect. Biol.* **16**, a041445 (2024).
5. D. S. Lu *et al.*, Reticulate evolution and rapid development of reproductive barriers upon secondary contact pose challenges for species delineation in a forest fungus. *Curr. Biol.* **34**, 4513–4525 (2024).
6. J. A. Coyne, H. A. Orr, Patterns of speciation in *Drosophila*. *Evolution (N.Y.)* **43**, 362–381 (1989).
7. S. Gourbière, J. Mallet, Are species real? The shape of the species boundary with exponential failure, reinforcement, and the "missing snowball." *Evolution (N.Y.)* **64**, 1–24 (2010).
8. J. M. Coughlan, D. R. Matute, The importance of intrinsic postzygotic barriers throughout the speciation process: Intrinsic barriers throughout speciation. *Philos. Trans. R. Soc. Lond. B Biol. Sci.* **375**, 201990533 (2020).
9. B. Reatini, T. J. Vision, The two faces of secondary contact on islands: Introgressive hybridization between endemics and reproductive interference between endemics and introduced species. *J. Biogeogr.* **51**, 483–498 (2024).
10. S. Edmands, Does parental divergence predict reproductive compatibility? *Trends Ecol. Evol.* **17**, 520–527 (2002).
11. E. B. Taylor *et al.*, Speciation in reverse: Morphological and genetic evidence of the collapse of a three-spined stickleback (*Gasterosteus aculeatus*) species pair. *Mol. Ecol.* **15**, 343–355 (2006).
12. J. A. McGuire *et al.*, Species delimitation, phylogenomics, and biogeography of Sulawesi flying lizards: A diversification history complicated by ancient hybridization, cryptic species, and arrested speciation. *Syst. Biol.* **72**, 885–991 (2023).
13. P. R. Grant, B. R. Grant, The secondary contact phase of allopatric speciation in Darwin's finches. *Proc. Natl. Acad. Sci. U.S.A.* **106**, 20141–20148 (2009).
14. E. J. Richards, C. H. Martin, Adaptive introgression from distant Caribbean islands contributed to the diversification of a microendemic adaptive radiation of trophic specialist pupfishes. *PLoS Genet.* **13**, 1–35 (2017).
15. M. Schumer, R. Cui, G. G. Rosenthal, P. Andolfatto, Reproductive isolation of hybrid populations driven by genetic incompatibilities. *PLoS Genet.* **11**, 1–21 (2015).
16. K. S. Pfennig, D. W. Pfennig, Character displacement: Ecological and reproductive responses to a common evolutionary problem. *Q. Rev. Biol.* **84**, 253–276 (2009).
17. D. R. Matute, B. S. Cooper, Comparative studies on speciation: 30 years since Coyne and Orr. *Evolution (N.Y.)* **75**, 764–778 (2021).
18. R. Yukilevich, Reproductive character displacement drives diversification of male courtship songs in *Drosophila*. *Am. Nat.* **197**, 690–707 (2021).
19. C. Dufresnes *et al.*, Mass of genes rather than master genes underlie the genomic architecture of amphibian speciation. *Proc. Natl. Acad. Sci. U.S.A.* **118**, e2103963118 (2021).
20. S. Singhal, C. Moritz, Reproductive isolation between phylogeographic lineages scales with divergence. *Proc. R. Soc. B Biol. Sci.* **280**, 20132246 (2013).
21. C. Roux *et al.*, Shedding light on the grey zone of speciation along a continuum of genomic divergence. *PLoS Biol.* **14**, 1–22 (2016).
22. P. Nosil, J. L. Feder, S. M. Flaxman, Z. Gompert, Tipping points in the dynamics of speciation. *Nat. Ecol. Evol.* **1**, 1–8 (2017).
23. J. V. Peñalba, L. Joseph, C. Moritz, Current geography masks dynamic history of gene flow during speciation in northern Australian birds. *Mol. Ecol.* **28**, 630–643 (2019).
24. R. Yamaguchi, Y. Iwasa, A tipping point in parapatric speciation. *J. Theor. Biol.* **421**, 81–92 (2017).
25. M. Vences, A. Miralles, C. Dufresnes, Next-generation species delimitation and taxonomy: Implications for biogeography. *J. Biogeogr.* **52**, 1–14 (2024).
26. A. J. Geneva, J. Hilton, S. Noll, R. E. Glor, Multilocus phylogenetic analyses of Hispaniolan and Bahamian trunk anoles (*distichus* species group). *Mol. Phylogenet. Evol.* **87**, 105–117 (2015).
27. R. S. Thorpe, Y. Surget-Groba, H. Johansson, Genetic tests for ecological and allopatric speciation in anoles on an island archipelago. *PLoS Genet.* **6**, e1000929 (2010).
28. R. J. Whittaker, J. M. Fernández-Palacios, T. J. Matthews, M. K. Borregaard, K. A. Triantis, Island biogeography: Taking the long view of nature's laboratories. *Science* **357**, eaam8326 (2017).
29. J. B. Losos, R. E. Ricklefs, Adaptation and diversification on islands. *Nature* **457**, 830–836 (2009).
30. A. M. S. Nugraha, R. Hall, Late cenozoic palaeogeography of Sulawesi, Indonesia. *Palaeogeogr. Palaeoclimatol. Palaeoecol.* **490**, 191–209 (2018).
31. B. J. Evans *et al.*, Monkeys and toads define areas of endemism on Sulawesi. *Evolution (N.Y.)* **57**, 1436–1443 (2003).
32. B. G. Kuhnhäuser *et al.*, Island geography drives evolution of rattan palms in tropical Asian rainforests. *Science* **387**, 1204–1209 (2025).
33. D. J. Lohman *et al.*, Biogeography of the Indo-Australian archipelago. *Annu. Rev. Ecol. Evol. Syst.* **42**, 205–226 (2011).
34. B. J. Evans *et al.*, Speciation over the edge: Gene flow among non-human primate species across a formidable biogeographic barrier. *R. Soc. Open Sci.* **4**, 170351 (2017).
35. I. F. Mandagi *et al.*, Species divergence and repeated ancient hybridization in a Sulawesian lake system. *J. Evol. Biol.* **34**, 1767–1780 (2021).
36. S. D. Howard, G. R. Gillespie, A. Riyanto, D. T. Iskandar, A new species of large *Eutropis* (Scincidae) from Sulawesi, Indonesia. *J. Herpetol.* **41**, 604–610 (2007).
37. A. A. T. Amarasinghe *et al.*, Systematic composition of the *Eutropis multifasciata* (Kuhl 1820) species complex (Squamata: Scincidae) and designation of a neotype. *Herpetologica* **74**, 342–354 (2018).
38. B. R. Karin *et al.*, Elevational surveys of Sulawesi herpetofauna 1: Gunung Galang, Gunung Dako Nature Reserve. *PeerJ* **11**, 1–19 (2023).
39. A. Datta-Roy, M. Singh, C. Srinivasulu, K. P. Karanth, Phylogeny of the Asian *Eutropis* (Squamata: Scincidae) reveals an 'into India' endemic Indian radiation. *Mol. Phylogenet. Evol.* **63**, 817–824 (2012).
40. A. J. Barley, A. Datta-Roy, K. P. Karanth, R. M. Brown, Sun skink diversification across the Indian-Southeast Asian biogeographical interface. *J. Biogeogr.* **42**, 292–304 (2015).
41. B. R. Karin, T. Gamble, T. R. Jackman, Optimizing phylogenomics with rapidly evolving long exons: Comparison with anchored hybrid enrichment and ultraconserved elements. *Mol. Biol. Evol.* **37**, 904–922 (2020).
42. D. Kornai, X. Jiao, J. Ji, T. Flouri, Z. Yang, Hierarchical heuristic species delimitation under the multispecies coalescent model with migration. *Syst. Biol.* **73**, 1015–1037 (2024).
43. X. X. Pang, D. Y. Zhang, Impact of ghost introgression on coalescent-based species tree inference and estimation of divergence time. *Syst. Biol.* **72**, 35–49 (2023).
44. B. J. Evans *et al.*, Speciation over the edge: Gene flow among non-human primate species across a formidable biogeographic barrier. *R. Soc. Open Sci.* **4**, 170351 (2017).
45. B. J. M. Jarrett, P. A. Downing, E. I. Svensson, Meta-analysis reveals that phenotypic plasticity and divergent selection promote reproductive isolation during incipient speciation. *Nat. Ecol. Evol.* **9**, 833–844 (2025).
46. J. Q. Richmond, E. L. Jockusch, A. M. Latimer, Mechanical reproductive isolation facilitates parallel speciation in western North American scincid lizards. *Am. Nat.* **178**, 320–332 (2011).
47. J. Q. Richmond *et al.*, Genomic discordance throws a wrench in the parallel speciation hypothesis for scincid lizards. *Evolution (N.Y.)* **79**, 1386–1399 (2025).
48. M. R. Servedio, M. A. F. Noor, The role of reinforcement in speciation: Theory and data. *Annu. Rev. Ecol. Evol. Syst.* **34**, 339–364 (2003).
49. E. J. Richards, M. R. Servedio, C. H. Martin, Searching for sympatric speciation in the genomic era. *BioEssays* **41**, 1–10 (2019).
50. D. R. Matute, Reinforcement can overcome gene flow during speciation in *Drosophila*. *Curr. Biol.* **20**, 2229–2233 (2010).
51. F. Roda, F. K. Mendes, M. W. Hahn, R. Hopkins, Genomic evidence of gene flow during reinforcement in Texas *Phlox*. *Mol. Ecol.* **26**, 2317–2330 (2017).
52. E. Mayr, Wallace's Line in the light of recent zoogeographic studies. *Q. Rev. Biol.* **19**, 1–14 (1944).

53. B. R. Karin, I. Das, T. R. Jackman, A. M. Bauer, Ancient divergence time estimates in *Eutropis rugifera* support the existence of Pleistocene barriers on the exposed Sunda Shelf. *PeerJ* **2017**, e3762 (2017).
54. D. W. Pfennig, K. S. Pfennig, Character displacement. *Curr. Biol.* **30**, R1023–R1024 (2020).
55. L. De Meester, J. Vanoverbeke, L. J. Kilsdonk, M. C. Urban, Evolving perspectives on monopolization and priority effects. *Trends Ecol. Evol.* **31**, 136–146 (2016).
56. B. Q. Minh *et al.*, IQ-tree 2: New models and efficient methods for phylogenetic inference in the genomic era. *Mol. Biol. Evol.* **37**, 1530–1534 (2020).
57. S. Kalyaanamoorthy, B. Q. Minh, T. K. F. Wong, A. Von Haeseler, L. S. Jermiin, ModelFinder: Fast model selection for accurate phylogenetic estimates. *Nat. Methods* **14**, 587–589 (2017).
58. R. W. Bryson *et al.*, A phylogenomic perspective on the biogeography of skinks in the *Plestiodon brevirostris* group inferred from target enrichment of ultraconserved elements. *J. Biogeogr.* **44**, 2033–2044 (2017).
59. S. B. Reilly *et al.*, Diverge and Conquer: Phylogenomics of southern Wallacean forest skinks (Genus: *Sphenomorphus*) and their colonization of the Lesser Sunda Archipelago. *Evolution (N.Y.)* **76**, 1–21 (2022), 10.1111/evo.14592.
60. J. G. Bragg *et al.*, Phylogenomics of a rapid radiation: The Australian rainbow skinks. *BMC Evol. Biol.* **18**, 1–12 (2018).
61. J. J. Wiens *et al.*, Resolving the phylogeny of lizards and snakes (Squamata) with extensive sampling of genes and species. *Biol. Lett.* **8**, 1043–1046 (2012).
62. C. R. Hutter *et al.*, FrogCap: A modular sequence capture probe-set for phylogenomics and population genetics for all frogs, assessed across multiple phylogenetic scales. *Mol. Ecol. Resour.* **22**, 1100–1119 (2022).
63. A. Stamatakis, RAxML version 8: A tool for phylogenetic analysis and post-analysis of large phylogenies. *Bioinformatics* **30**, 1312–1313 (2014).
64. C. Zhang, S. Mirarab, Weighting by gene tree uncertainty improves accuracy of quartet-based species trees. *Mol. Biol. Evol.* **39**, 1–22 (2022).
65. J. K. Pritchard, M. Stephens, P. Donnelly, Inference of population structure using multilocus genotype data. *Genetics* **155**, 945–959 (2000).
66. T. Flouri, X. Jiao, J. Huang, B. Rannala, Z. Yang, Efficient Bayesian inference under the multispecies coalescent with migration. *Proc. Natl. Acad. Sci. U.S.A.* **120**, 1–11 (2023).
67. R. Nielsen, J. Wakeley, Distinguishing migration from isolation: A Markov chain Monte Carlo approach. *Genetics* **158**, 885–896 (2001).
68. E. A. Chambers *et al.*, Distinguishing species boundaries from geographic variation. *Proc. Natl. Acad. Sci. U.S.A.* **122**, e2423688122 (2025).
69. N. D. Jackson, B. C. Carstens, A. E. Morales, B. C. O'Meara, Species delimitation with gene flow. *Syst. Biol.* **66**, 799–812 (2017).
70. H. Shang *et al.*, Phytop: A tool for visualizing and recognizing signals of incomplete lineage sorting and hybridization using species trees output from ASTRAL. *Hortic. Res.* **12**, uhae330 (2025).
71. M. Malinsky, M. Matschiner, H. Svardal, Dsuite – Fast D-statistics and related admixture evidence from VCF files. *Mol. Ecol. Resour.* **21**, 584–595 (2021).
72. C. Solís-Lemus, P. Bastide, C. Ané, PhyloNetworks: A package for phylogenetic networks. *Mol. Biol. Evol.* **34**, 3292–3298 (2017).
73. D. Wen, Y. Yu, J. Zhu, L. Nakhleh, Inferring phylogenetic networks using PhyloNet. *Syst. Biol.* **67**, 735–740 (2018).
74. J. Ji, D. J. Jackson, A. D. Leache, Z. Yang, Power of bayesian and heuristic tests to detect cross-species introgression with reference to gene flow in the *Tamias quadrivittatus* group of North American chipmunks. *Syst. Biol.* **72**, 446–465 (2023).
75. G. P. Tiley *et al.*, Estimation of species divergence times in presence of cross-species gene flow. *Syst. Biol.* **72**, 820–836 (2023).
76. S. B. Reilly *et al.*, Phylogenomic analysis reveals dispersal-driven speciation and divergence with gene flow in Lesser Sunda flying lizards (genus *Draco*). *Syst. Biol.* **71**, 221–241 (2022).
77. L. A. Bergeron *et al.*, Evolution of the germline mutation rate across vertebrates. *Nature* **615**, 285–291 (2023).
78. D. M. Portik, J. J. Wiens, SuperCRUNCH: A bioinformatics toolkit for creating and manipulating supermatrices and other large phylogenetic datasets. *Methods Ecol. Evol.* **11**, 763–772 (2020).
79. R. Bouckaert *et al.*, BEAST 2.5: An advanced software platform for Bayesian evolutionary analysis. *PLoS Comput. Biol.* **15**, 1–28 (2019).
80. B. R. Karin, M. Metallinou, J. L. Weinell, T. R. Jackman, A. M. Bauer, Resolving the higher-order phylogenetic relationships of the circumtropical *Mabuya* group (Squamata: Scincidae): An out-of-Asia diversification. *Mol. Phylogenet. Evol.* **102**, 220–232 (2016).
81. N. J. Matzke, Model selection in historical biogeography reveals that founder-event speciation is a crucial process in island clades. *Syst. Biol.* **63**, 951–970 (2014).
82. S. Meiri, SquamBase–A database of squamate (Reptilia: Squamata) traits. *Glob. Ecol. Biogeogr.* **33**, 1–13 (2024).
83. L. J. Revell, Phytools 2.0: An updated R ecosystem for phylogenetic comparative methods (and other things). *PeerJ* **12**, e16505 (2024).
84. P. Bastide, C. Solís-Lemus, R. Kriebel, K. William Sparks, C. Ané, Phylogenetic comparative methods on phylogenetic networks with reticulations. *Syst. Biol.* **67**, 800–820 (2018).
85. B. R. Karin, Datasets for: When Islands Collide: Divergence predicts outcomes of secondary contact during the fusion of Sulawesi's Paleo-Archipelago. Zenodo (2025), 10.5281/zenodo.17193122 [Deposited 25 Sep 2025].
86. B. R. Karin, SRA Dataset: When Islands Collide: Divergence predicts outcomes of secondary contact during the fusion of Sulawesi's Paleo-Archipelago. https://www.ncbi.nlm.nih.gov/sra/PRJNA1333612 [Deposited 25 Sep 2025].